Ising model with competing next-nearest-neighbour interactions on the Kagome lattice

1988 J. Phys. A: Math. Gen. 21 2195

(http://iopscience.iop.org/0305-4470/21/9/032)

J. Phys. A: Math. Gen. **21** (1988) 2195-2209. Printed in the UK

Ising model with competing next-nearest-neighbour interactions on the Kagome lattice

M Wolf and K D Schotte

Institut für Theoretische Physik, Freie Universität Berlin, Arnimallee 14, D-1000 Berlin 33, Federal Republic of Germany

Received 29 October 1987

Abstract. Starting from a model for $CsOH.H_2O$ we investigate the phase diagram of a two-dimensional Ising model on the Kagome lattice with antiferromagnetic nearest-neighbour and competing ferromagnetic second- and third-nearest-neighbour interactions by Monte Carlo simulations. We obtain two Kosterlitz-Thouless transitions as in the six-state clock model and a crossover to second-order transitions where the critical exponents are consistent with those of the three-state Potts model. We also determine the ground state for all values of the coupling constants.

1. Introduction

There are many crystals with two-dimensional hydrogen bonding (Matsuo and Suga 1981). One example is $CsOH.H_2O$ (caesium hydroxide monohydrate), which crystallises in layers of alternating Cs^+ ions and nets of $H_3O_2^-$, almost identical to normal hexagonal ice (Stahn *et al* 1983). The oxygens form a honeycomb lattice with the protons sitting on two positions between them as in ordinary ice. If we connect the mean positions of neigbouring hydrogens, we obtain a Kagome lattice. The two positions can then be represented by an Ising spin, which is shown in figure 1. Since one expects the protons to disorder even at moderate temperature, an antiferromagnetic nearest-neighbour (NN) coupling should be the dominant one. This excludes also the H_3O^+, O^{2-} configurations at low temperatures, which are not observed experimentally.

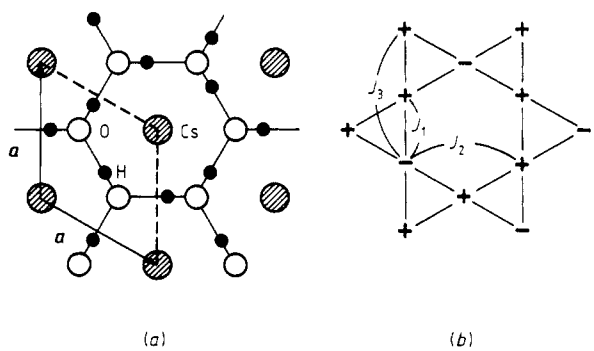

Figure 1. (*a*) $CsOH.H_2O$, projected into the a-a-plane. Open circles (○) refer to the oxygens and full ones (●) to the hydrogens. The Cs^+ ions are located at $\frac{1}{2}c$ between two $H_3O_2^-$ layers. (*b*) Conversion into an Ising model. J_1, J_2, J_3 denote the nearest- and next-nearest-neighbour interactions.

The Kagome-Ising antiferromagnet (KAF), first investigated by Kano and Naya (1953), is like the triangular case disordered at all temperatures, but possesses a much larger zero-point entropy per spin of $0.502k$ as compared to Wannier's result of $0.338k$ for the triangular lattice (Wannier 1950). Sütö has noticed that the KAF is 'superfrustrated', which means that the correlation function at $T=0$ decays exponentially in contrast to the algebraic decay in the triangular case (Sütö 1981). The KAF has obviously no phase transition and would be only a poor model for $CsOH.H_2O$. It is of course possible to choose anisotropic antiferromagnetic coupling constants; however, this destroys the symmetry. Therefore we will introduce next-nearest-neighbour (NNN) interactions and consider the Hamiltonian

$$H = -J_1 \sum_{\mathrm{NN}} \sigma_i\sigma_j - J_2 \sum_{\mathrm{NNN}_2}^{\text{Kagome}} \sigma_i\sigma_j - J_3 \sum_{\mathrm{NNN}_3}^{\text{square}} \sigma_i\sigma_j \tag{1}$$

where $\sigma_i = \pm 1$ and the sums run over NN and NNN pairs, as indicated in figure 1. As pointed out, we consider antiferromagnetic NN coupling $J_1 < 0$. The 'Kagome' refers to the second-neighbour interaction J_2, which couples the spins of each of three Kagome sublattices. The 'square' refers to the third-neighbour coupling J_3 on each of three rhombic square sublattices. Considering the distances between the protons in figure 1, we expect, that both J_2 and J_3 will be ferromagnetic ($J_2, J_3 > 0$).

As has been pointed out before in the case of the triangular lattice by several authors (Kanamori 1985 and references therein, Brand and Stolze 1986), we will find a rich structure of possible ground states. Varying the temperature in a Monte Carlo procedure, we obtain in the special cases of zero J_2 or J_3 coupling two Kosterlitz-Thouless transitions. As we will show, in this case our model belongs to the universality class of the six-state clock model. In the case of antiferromagnetic NN and ferromagnetic NNN coupling on the triangular lattice, such behaviour has also been observed (Landau 1983). Since the J_2 and J_3 couplings favour ordering on two different types of sublattices of a frustrated system, they are competing with each other and we get crossover effects. If $J_2 = J_3$, the ground state is infinite degenerate and can be described by a modified KDP model. But there is still some order, which gives rise to a three state Potts transition at a non-zero critical temperature. In the next section we determine the ground states for all possible coupling constants and discuss the special case where $J_2 = J_3$ in the following section. Then we come back to thermodynamics, which is studied by the Monte Carlo method and analysed by finite-size scaling.

2. Ground states

To obtain the ground states of our model, we will use a method first introduced by Kanamori (1966), which has been taken up and modified by other authors (Brandt and Stolze 1986). Here we will follow the notation of Brandt and Stoke. We first rewrite the Hamiltonian (1) as

$$H = 2N\left[-J_1\left(\frac{1}{2N}\sum_{\mathrm{NN}}\sigma_i\sigma_j\right) - J_2\left(\frac{1}{2N}\sum_{\mathrm{NNN}_2}\sigma_i\sigma_j\right) - J_3\left(\frac{1}{2N}\sum_{\mathrm{NNN}_3}\sigma_i\sigma_j\right)\right]$$

to obtain

$$H = 2N(-J_1c_1 - J_2c_2 - J_3c_3). \tag{2}$$

Now the energy is a linear function of the two-spin correlation coefficients c_1, c_2 and c_3. Of course by definition the coefficients c_i are restricted by

$$-1 \leqslant c_i \leqslant +1 \qquad i = 1, 2, 3. \tag{3}$$

In the next step we construct more efficient restrictions, which are linear inequalities of the type

$$b \leqslant a_1 c_1 + a_2 c_2 + a_3 c_3 \tag{4}$$

where the coefficients a_i and b are given in table 1.

There is a systematic way to find these inequalities; however it is also a procedure of trial and error, as we will illustrate shortly. In order to understand inequality 1 we consider a small cluster of three NN spins σ_1, σ_2 and σ_3 in a triangle. Obviously one finds

$$-1 \leqslant \sigma_1\sigma_2 + \sigma_2\sigma_3 + \sigma_3\sigma_1 \leqslant 3 \tag{5}$$

for the two cases of ferro- and antiferromagnetic arrangement. Summing over all triangles in the lattice as before in the Hamiltonian, we get

$$-1 \leqslant 3c_1 \leqslant 3. \tag{6}$$

The first inequality is number 1, the second turns out to be superfluous, since other inequalities in our list are stronger. Now we can arrange three spins in a row and obtain again from (5)

$$-1 < \pm 2c_1 + c_3 \tag{7}$$

where c_3 comes from the summation over all J_3 bonds. Again one can throw away the inequality with + and that with the − gives inequality 4. The most complicated cluster that we had to consider consists of two triangles sharing one corner (inequalities 6 and 7). Geometrically the ten inequalities in table 1 generate a three-dimensional convex polyhedron. For allowed energies equation (2) describes a plane which cuts the polyhedron. The energy reaches its extreme values if the plane just touches one corner of the polyhedron. If it touches an edge, there is a phase boundary. The inequalities in table 1 lead to nine corners of the polyhedron, which are listed in table 2.

Table 1. Coefficients a_i $(i = 1, 2, 3)$ and b of equation (4).

Inequality	b	a_1	a_2	a_3
1	−1	3	0	0
2	−1	0	3	0
3	−1	−2	1	0
4	−1	−2	0	1
5	−1	2	0	1
6	−1	3	1	1
7	−1	−1	1	1
8	−1	1	−1	−1
9	−1	−1	1	−1
10	−1	−1	−1	1

Table 2. The parameters c_i $(i = 1, 2, 3)$ and structure of the nine corners of the polyhedron derived from the inequalities of table 1.

Corner	c_1	c_2	c_3	Structure
1	1	1	1	(1×1)
2	$-\frac{1}{3}$	1	$-\frac{1}{3}$	$(\sqrt{3}\times\sqrt{3})$
3	$-\frac{1}{3}$	$-\frac{1}{3}$	1	(1×1)
4	0	0	-1	(2×2)
5	0	$-\frac{1}{3}$	$-\frac{2}{3}$	(2×4)
6	$-\frac{1}{3}$	$-\frac{1}{3}$	$\frac{1}{3}$	(1×2)
7	$-\frac{1}{3}$	$\frac{1}{3}$	$-\frac{1}{3}$	(1×2)
8	$\frac{1}{3}$	$-\frac{1}{3}$	$\frac{1}{3}$	(2×1)
9	$\frac{1}{3}$	$-\frac{1}{3}$	$-\frac{1}{3}$	(2×1)

The main problem is now to find a spin configuration, which corresponds to the calculated values of the c_i. Now it could turn out that it is impossible to find a spin structure for some corners. Then one has to construct stronger inequalities which eliminate these fictitious corners. Systematically one starts with small clusters and ends with bigger ones. Figure 2 shows the phases corresponding to the corners in table 2. Now it is easy to obtain the phase diagram by considering (2). For both positive and negative J_1 only seven phases appear, as one can see in figure 3.

As we have pointed out in § 1, we are interested in antiferromagnetic J_1 coupling and smaller ferromagnetic J_2 and J_3 couplings. If then J_2 dominates, we get ground state number 2, which is characterised by ferromagnetic ordering on the three Kagome sublattices and by the frustration condition for the NN triangles. Analogously we obtain the ground state number 3, if J_3 dominates and we now have ferromagnetic ordering on the three square sublattices. Both ground states are sixfold degenerate. As we will see later, this is connected to the appearance of a critical behaviour as in the six-state clock model.

3. Phase boundary $J_2 = J_3$

As is well known, competing interactions in Ising models can give rise to infinite degenerate ground states and modulated phases (see Yeomans 1984 and references therein). The most prominent case is that of the ANNNI model. In our case where $J_2 = J_3 > 0$ and $J_1 < 0$ the phases 2 and 3 can be mixed in such a way that the domain boundaries cost no energy. At first sight this problem looks very complicated, since we have to match different spin patterns. The problem can be simplified by an argument similar to the two-dimensional ANNNI model (Villain and Bak 1981).

Let us start with phase 2 (see figure 2) and turn around all negative spins in order to obtain a ferromagnet. Since the reversed spins form a regular lattice, it is possible to flip them also in phase 3. As can be seen in figure 4 one obtains lines connecting negative spins all running in one main direction. To complete the argument one must find out how much energy such a line costs. We observe that for $J_2 = J_3$ the line energy is zero. However, they could end at the boundary between domains of phase 2 and phase 3. This ending of lines, and also the crossing of lines, cost energies of the order of J_2 or J_3, as one can calculate. So the ground state in this coexistence regime can be understood as a ferromagnet disordered by non-crossing lines of reversed spins,

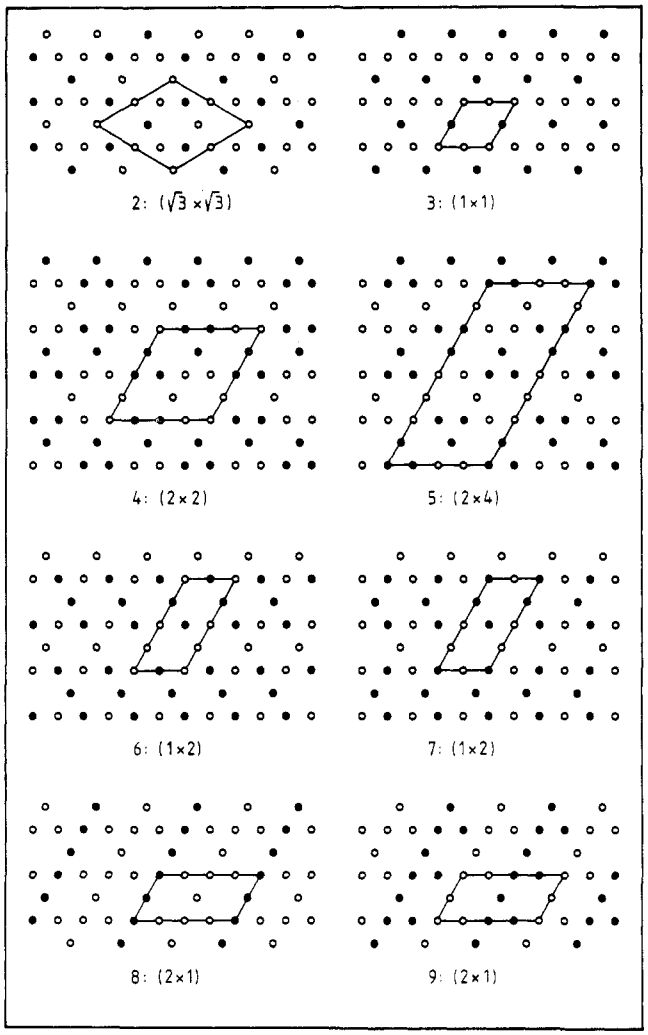

Figure 2. Spin configurations corresponding to the corners 2-9 listed in table 2. Open circles (○) represent the + spins and full circles (●) the − spins. The unit cells are indicated.

which do not end. Indeed cooling in the Monte Carlo procedure leads to such typical configurations for $J_2 = J_3$ at low temperatures. The same argument is valid, if we start with phase 3 as the fictitious ferromagnet, when we then get the same lines as for phase 2. The disordered lines look somewhat like a graphical representation of the ice model on the square lattice (Lieb and Wu 1972). Since the lines cost no energy, all vertices have the same weight. Only vertices with crossing lines cost energy, which can be set equal to infinity for low-temperature investigations.

It is not sufficient to keep J_2 equal to J_3 to obtain a phase diagram at low temperatures. Depending on the distance between lines, the line energy ε varies between $8|J_2 - J_3|$ and $12|J_2 - J_3|$. So the mapping onto an ice model is not completely rigorous. In order to proceed, we take the average value $\varepsilon = 10|J_2 - J_3|$ and make the identifications with the vertex weights of the modified KDP model (Wu 1967) as in

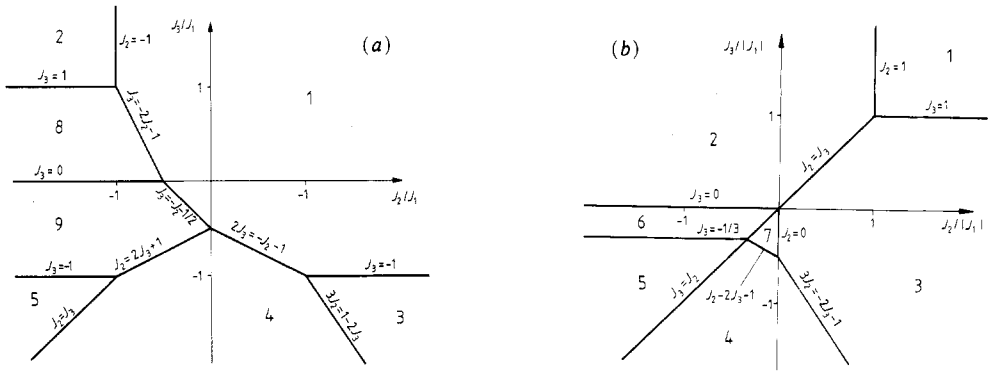

Figure 3. Ground-state phase diagram for (*a*) $J_1>0$ and (*b*) $J_2<0$. The numbers in the different regions refer to the corners represented in figure 2.

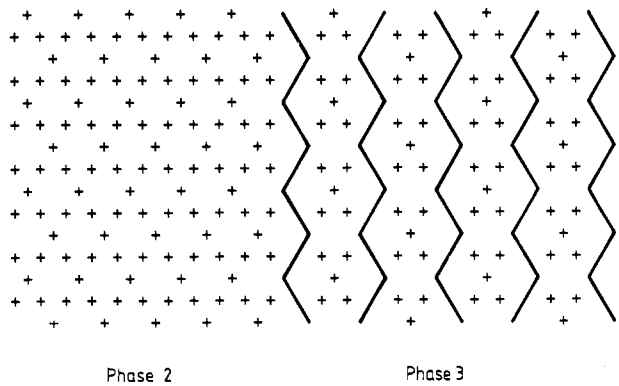

Figure 4. Phase boundary between phase 2 and phase 3 (see figure 2). All spins of one Kagome sublattice have been reversed in both phases as explained in the text. Negative neighbouring spins are connected by the bold lines.

figure 5. From Lieb and Wu (1972), we find that the zero-point entropy in the case of $J_2=J_3$ is

$$\frac{S(0)}{kN_V}=\frac{1}{4\pi}\int_{-\pi}^{\pi}d\theta\,\ln[\max\{1,2(1-\cos\theta)\}]=0.324 \tag{8}$$

where N_V is the number of vertices, which is just $N/3$. So the entropy per spin is only $\frac{1}{3}$ of the value above. At non-zero ε we have ordering in either phase 2 or phase 3 and the transition temperature is given by $T_c=\varepsilon/\ln 2$. This conclusion is not so reliable, because of the difficulties mentioned above and is restricted to low temperature. But we think it is qualitatively correct.

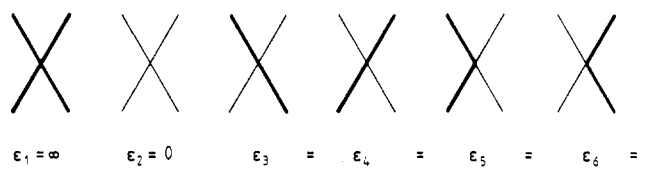

Figure 5. Vertex weights of the modified KDP model.

Since we have for $J_2 = J_3$ a very little entropy per spin of $0.108k$ compared to the KAF value of $0.502k$ cited before, it is not surprising that there is another phase transition at higher temperature. The vertices can be placed on one of three square sublattices, which is equivalent to choosing three main directions for the disordered lines. The three-state Potts model and the hard-hexagon model have also such an internal three-fold symmetry. The critical exponents found in the Monte Carlo simulations are in agreement with this reasoning and for $J_2 = J_3$ our model belongs to the same universality class as the three-state Potts model. For details we refer to § 4.

4. Finite-temperature study

4.1. Order parameter and Monte Carlo method

We study the specific heat and the sublattice magnetisation by a Monte Carlo procedure (see Binder 1979). Since there are three sublattices, there is some ambiguity to define the order parameter. We find it convenient to use the following one,

$$m = \tfrac{1}{3}(|M_1| + |M_2| + |M_3|) \tag{9}$$

where the M_i denote the sublattice magnetisation per spin. If J_2 dominates, we measure the magnetisation on the Kagome sublattices and if $J_3 > J_2$ we choose the square sublattices. For the finite-size scaling analysis we also calculate the high-temperature susceptibility per spin

$$\chi^+ = (N/3kT)(M_1^2 + M_2^2 + M_3^2) \tag{10}$$

where N is the number of spins. Together with the specific heat these quantities enable us to analyse the critical behaviour of our model. In the case $J_2 = J_3$, which we discussed in the last section, we calculated the total magnetisation M and the total susceptibility, which is given by the fluctuations of M.

We use a standard one-spin-flip importance sampling Monte Carlo procedure (see, e.g., Binder 1979). Up to 2000 Monte Carlo steps (MCS) per spin were omitted before we measured the thermodynamic quantities by averaging over 15 000–25 000 MCS per spin. We studied $N = 3 \times L \times L$ lattices with periodic boundary conditions for $6 \leqslant L \leqslant 72$. Tests of the program were made by comparing the Monte Carlo data with the exact values for the specific heat and the order parameter of a small system with $L = 3$. After cooling, the low-temperature spin configurations in the case $J_2 = J_3$ were printed out to control the argument in § 3.

4.2. Finite-size scaling

The key assertion of finite-size scaling is that the critical behaviour of the finite system of the length L is given in the critical region by the ratio $L/\xi(T)$, where $\xi(T)$ is the correlation length of the infinite system (see Barber 1982). A thermodynamic quantity like the susceptibility χ can be described near T_c by the scaling relation

$$\chi_L(T) = L^{\omega} Y_{\chi}(\xi(T)/L) \qquad L \to \infty \tag{11}$$

where ω is given by the ratio of critical exponents $\gamma/\nu = 2 - \eta$ and Y_{χ} is some unknown function. Now the critical temperature and also ω is not known *a priori*. To get an estimate one writes

$$\chi_L(T)/L^{\omega} = \chi_{L'}(T')/L'^{\omega} \tag{12}$$

which defines a mapping of the temperature $T \to T'$ (dos Santos and Sneddon 1981). At the critical temperature, where the correlation length diverges, there is a fixpoint of this mapping. Following Barber and Selke (1982) one plots

$$\xi_{LL'} = \ln(\chi_L/\chi_{L'})/\ln(L/L') \tag{13}$$

as a function of temperature for several L, L'. In the case of a second-order phase transition the curves $\xi_{LL'}$ intersect in one point, which determines an estimate of the critical temperature and the exponent ω. Now in the case of a Kosterlitz-Thouless transition like in the XY model, one has to take into account that the correlation length is given by

$$\xi(T) \sim \exp[a(T - T_c)^{-0.5}] \qquad \text{for } T > T_c \tag{14}$$

and remains infinite in the critical phase for $T < T_c$. In the case of a six-state clock model one has two Kosterlitz-Thouless transitions. As before we get the scaling relation (Challa and Landau 1986)

$$\chi_L = L^{2-\eta} \tilde{Y}_\chi\{L^{-1} \exp[a(T - T_2)^{-0.5}]\} \qquad \text{for } T > T_2. \tag{15}$$

For the lower transition at T_1 one gets a similar relation for the order parameter

$$m_L = L^{-\eta/2} \tilde{Y}_m\{L^{-1} \exp[a(T_1 - T)^{-0.5}]\} \qquad \text{for } T < T_1. \tag{16}$$

The critical exponent η is predicted to vary between the values of $\eta(T_1) = \frac{1}{9}$ and $\eta(T_2) = \frac{1}{4}$ and is non-universal (Jose *et al* 1977). In the critical phase, where $T_1 < T < T_2$, the correlation length is infinite and the curves $\xi_{LL'}$ of (13) should touch in this regime. This indicates a line of critical points and makes the Kosterlitz-Thouless behaviour easily visible (Barber 1982).

4.3. Results and discussion

As pointed out in § 1, we are interested in antiferromagnetic NN coupling ($J_1 < 0$) and smaller ferromagnetic NNN couplings ($J_2, J_3 > 0$). We therefore restrict the possible values of the coupling constants to the straight line in the J_1, J_2, J_3 parameter space, which is defined by $J_1 = -2(J_2 + J_3) = \text{constant}$. Finally we will get a temperature against $(J_2 - J_3)$ phase diagram, which is nearly symmetric around $J_2 = J_3$. So we show only the three cases $J_2 = 0$, $(J_3 - J_2) = \frac{1}{3}J$ and $J_2 = J_3$. All energies are given in units of $J = J_2 + J_3 = -\frac{1}{2}J_1$.

4.3.1. Critical behaviour for $J_2 = 0$. The Monte Carlo data for the specific heat and the order parameter in the case $J_2 = 0$ are shown in figure 6. The specific heat possesses two separated rounded peaks, which become nearly size independent for large L and we expect that the data for $L = 48$ lie very close to the values of the specific heat of the infinite system. In the temperature dependence of the order parameter we observe two 'shoulders', which are localised at temperatures where the specific heat has its two maxima. In the case $J_3 = 0$, which we do not show, we obtain qualitatively the same behaviour. Again the specific heat has two rounded maxima at temperatures lying slightly below.

In order to classify the critical behaviour we plot in figure 7(*a*) the $\xi_{LL'}$ of (13) for several L, L'. Within the statistical errors the curves touch each other below $kT^*/J \approx 3.2$, which indicates a Kosterlitz-Thouless transition at $T \approx T^*$ and the occurrence of a line of critical points for $T < T^*$. Since the system is ordered at low temperatures and

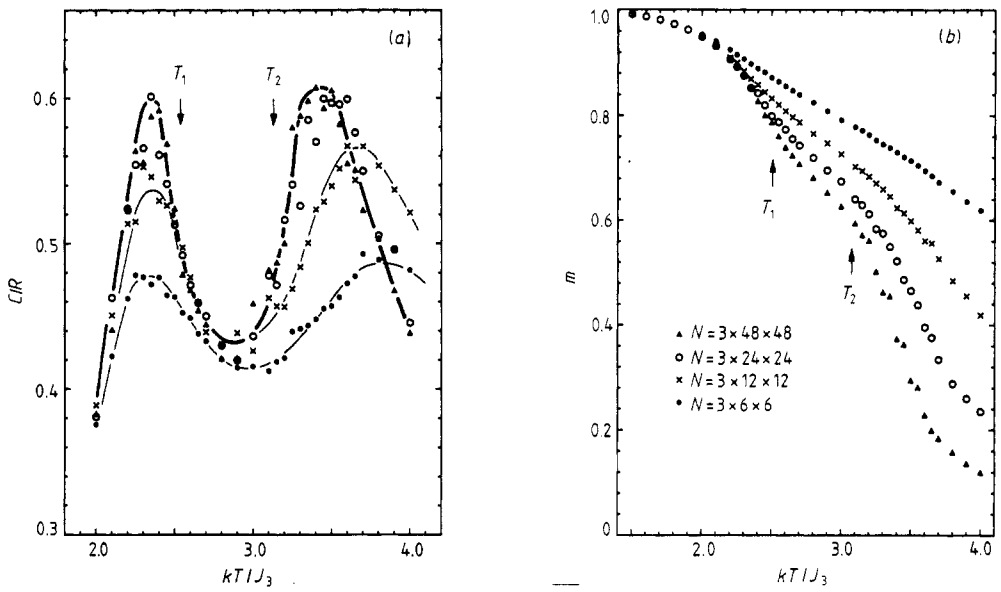

Figure 6. Temperature dependence of the specific heat (a) and the order parameter (b) for the case $J_2=0$, $J_1=-2J_3$. The bold curve in (a) refers to $N=3\times48\times48$.

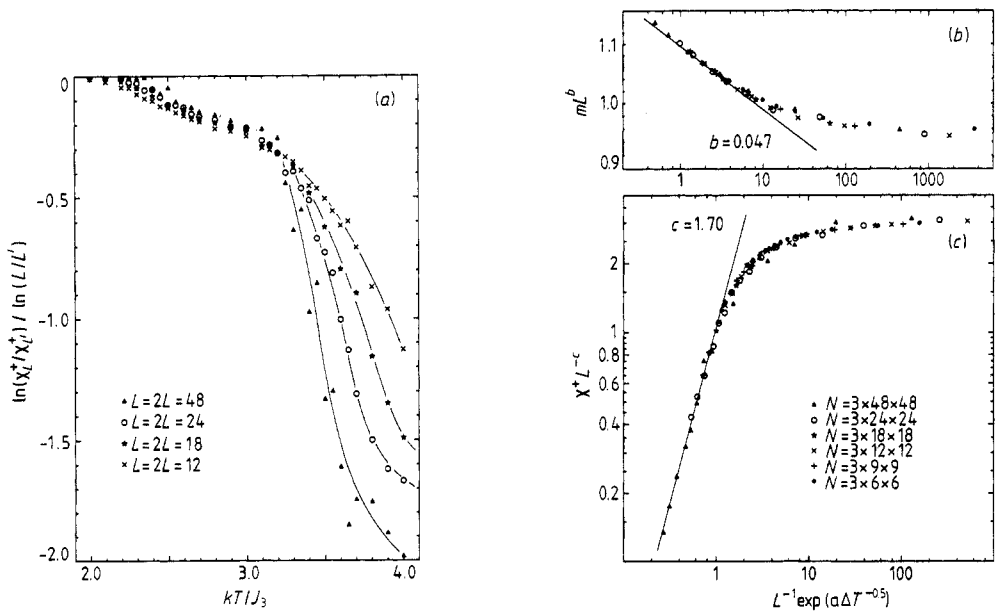

Figure 7. Plot of $\xi_{LL'}$ of (13) against temperature (a) for $J_2=0$ indicating a critical behaviour of the Kosterlitz–Thouless type. Finite-size scaling plots for $J_2=0$ of (b) the order parameter m with $b=\eta/2=0.047$ (see (16)) and (c) the high-temperature susceptibility χ with $c=2-\eta=1.70$ (see (15)).

the ground state is sixfold degenerate, we expect that there is another phase transition at lower temperatures as in the six-state clock model. As shown in figures 7(*b*) and (*c*) the data scale well according to (16) and (15) respectively. With errors estimated from the deviation of the results from the best fit, we obtain $a = 1.41 \pm 0.03$ and for the critical temperatures and exponents

$$kT_1/J|_{J_2=0} = 2.50 \pm 0.4 \qquad kT_2/J|_{J_2=0} = 3.07 \pm 0.05$$

$$\eta(T_1) = 0.10 \pm 0.01 \qquad \eta(T_2) = 0.30 \pm 0.03.$$

This shows that (13) gives qualitatively correct results but that the convergence of $T^* \to T_2$ for $L, L' \to \infty$ is very slow.

In the case $J_3 = 0$ we obtain the same critical behaviour and identical values of η. Our value for $\eta(T_2)$ differs slightly from the conjectured values $\eta(T_1) = \frac{1}{9}$ and $\eta(T_2) = \frac{1}{4}$ of the six-state clock model (Jose *et al* 1977), but the exponents are in agreement with the Monte Carlo results of Challa and Landau (1986), where $\eta(T_2) = 0.275 \pm 0.025$. We therefore conclude that for either $J_2 = 0$ or $J_3 = 0$ our model belongs to the universality class of the six-state clock model.

4.3.2. Crossover effects. We studied several cases varying the difference between J_2 and J_3. Decreasing $|J_2 - J_3|$ from J to $J/3$, the two maxima of the specific heat become merged. In the case $J_3 - J_2 = J/3$ (figure 8) the specific heat shows only one peak and we observe two regions in the finite-size behaviour of the order parameter. For temperatures below $kT/J \approx 1.5$ the order parameter is nearly size independent and falls off rapidly with increasing lattice size at higher temperatures. Figure 9 shows an intersection of the $\xi_{LL'}$ of (13) *at* $T^*/J \approx 1.55$, which indicates a second-order phase transition (Barber and Selke 1982). We estimate the critical temperature to be $kT_c/J = 1.50 \pm 0.05$.

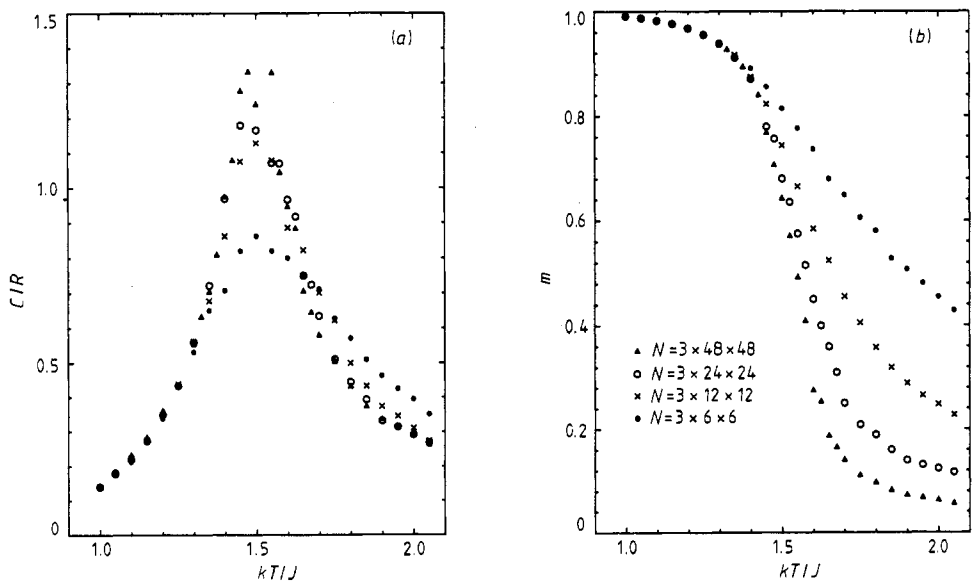

Figure 8. Temperature dependence of the specific heat (*a*) and the order parameter (*b*) for the case $J_3 - J_2 = J/3$.

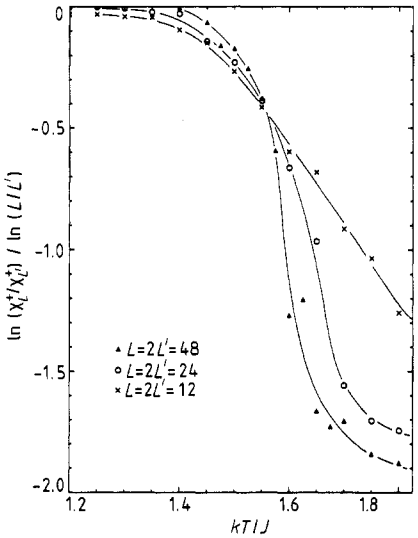

Figure 9. Plot of $\xi_{LL'}$ of (13) for the case $J_3 - J_2 = J/3$ indicating a second-order transition.

Starting with $|J_2 - J_3| = J$ ($J_2 = 0$ or $J_3 = 0$), we observed two Kosterlitz-Thouless transitions and a critical phase for $T_1 < T < T_2$. Decreasing $|J_2 - J_3|$ the transition temperatures T_1 and T_2 approach each other. The critical phase vanishes for $|J_2 - J_3| \approx J/3$ and the critical behaviour changes to second-order type.

4.3.3. Critical behaviour for $J_2 = J_3$. If $J_2 = J_3$ the ground state is infinitely degenerate and the is no ordering on the Kagome or square sublattices. We measure the total magnetisation M per spin, which approaches $\frac{1}{3}$ at low temperatures and decreases rapidly for temperatures higher than $kT/J \approx 0.82$ (figure 10). At this temperature the specific heat shows a very sharp peak and the susceptibility seems to diverge in the infinite system. Since we observed no hysteresis effects and metastability of M, we expect a second-order phase transition. In the critical region the thermodynamic quantities should then exhibit a power-law dependence of $|T - T_c|$. Assuming a critical behaviour $M \sim (T_c - T)^{\beta}$ for the magnetisation and $\chi \sim (T - T_c)^{-\gamma}$ for the suceptibility the least-squares fits for data with $L = 48$ and 72 lead to a critical temperature $T_c/J = 0.8207 \pm 0.0005$ and to the exponents (figures 11(a) and (b))

$$\beta = 0.12 \pm 0.01 \qquad \gamma = 1.54 \pm 0.07.$$

The assumption $E_c - E \sim (T_c - T)^{1-\alpha'}$ for $T < T_c$ and $E - E_c \sim (T - T_c)^{1-\alpha}$ for $T > T_c$ leads to a critical value of the energy $E_c/J = -1.885$ and to the exponents (figures 11(c) and (d))

$$\alpha' = 0.328 \pm 0.005 \qquad \alpha = 0.32v \pm 0.006.$$

Within the errors the relation $\alpha + 2\beta + \gamma = 2$ is fulfilled and the obtained critical exponents agree very well with the values $\alpha = \frac{1}{3}$, $\beta = \frac{1}{9}$ and $\gamma = \frac{13}{9}$ of the hard hexagon model, which belongs to the universality class of the three-state Potts model (Baxter 1982).

As we have pointed out in § 3, our model possesses for $J_2 = J_3$ a threefold symmetry and we therefore conclude that in this case our model belongs to the universality class of the three-state Potts model.

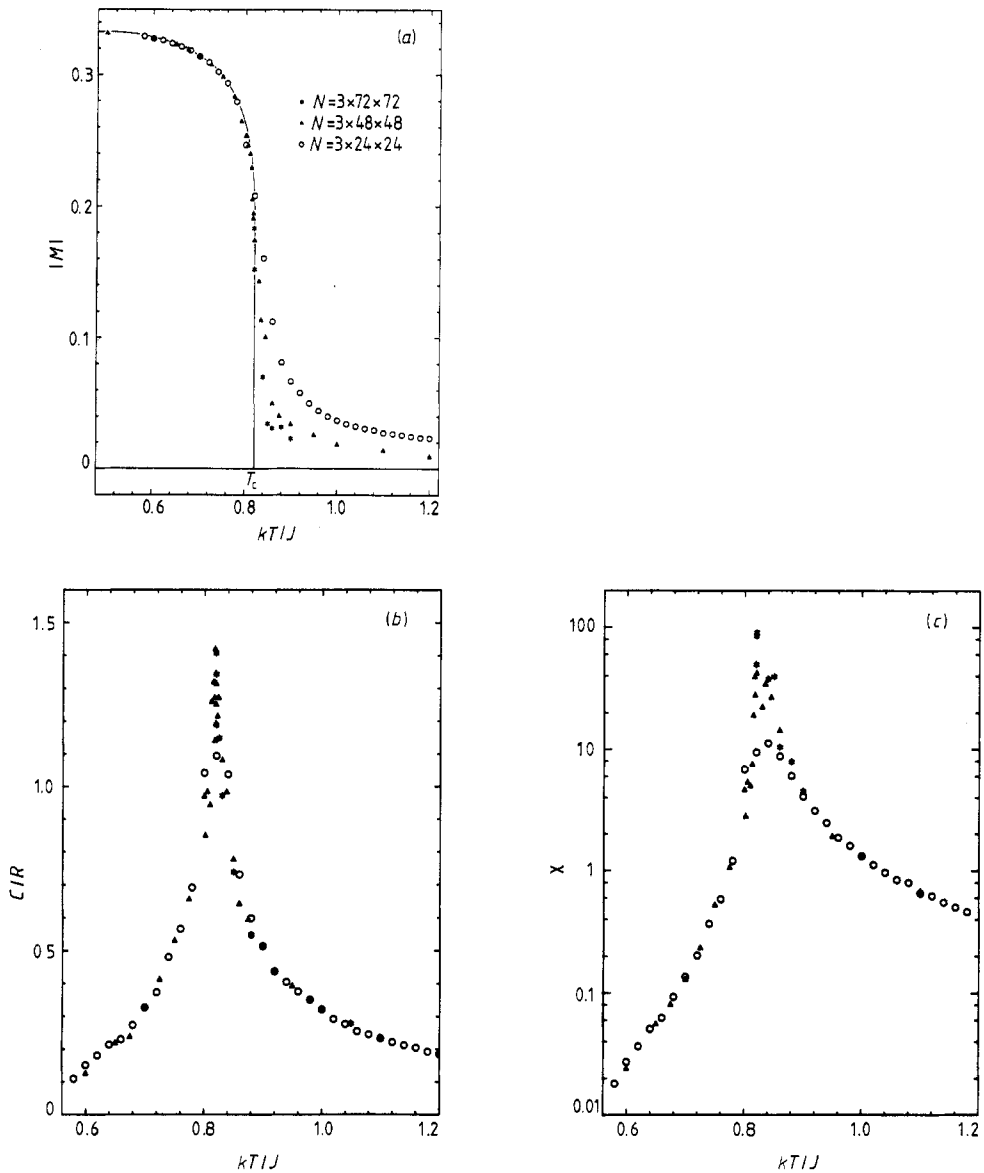

Figure 10. Temperature dependence of the total magnetisation (a), the specific heat (b) and the susceptibility (c) for the case $J_2 = J_3$. The curve in (a) shows the extrapolated behaviour of the infinite system.

4.4. Phase diagram

We can now summarise our results and we suggest for our model the phase diagram in figure 12 along the line $J_1 = -2(J_2 + J_3) = \text{constant}$. The phases 2 and 3 are very similar in a thermodynamic sense, which can be seen in the symmetry of the phase diagram. In the cases $|J_2 - J_3| = J$ we obtain a critical behaviour of the six-state clock and the crossover to second-order transitions is approxiately located at $|J_2 - J_3| = J/3$. As pointed out in § 3 there must be an intermediate phase between the phases 2 and 3,

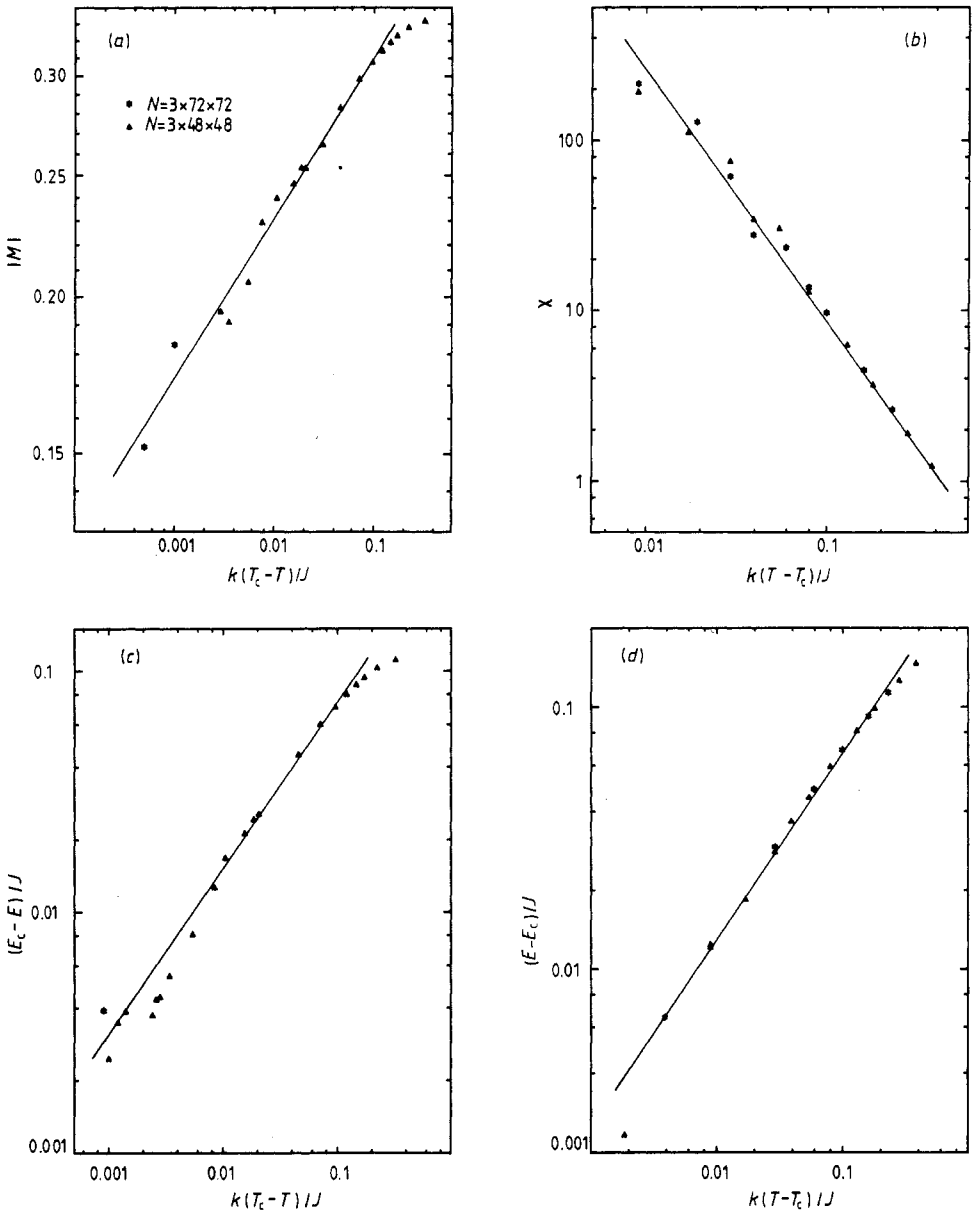

Figure 11. Least-square fits of the scaling laws for $J_2 = J_3$ for: (*a*) the total magnetisation m with $M \sim (T_c - T)^{\beta}$ and $\beta = 0.12$; (*b*) the susceptibility χ with $\chi \sim (T - T_c)^{-\gamma}$ and $\gamma = 1.54$; (*c*) the energy $(E_c - E)/J$ with $E_c - E \sim (T_c - T)^{1-\alpha'}$, $E_c = -1.885$ and $\alpha' = 0.33$; (*d*) the energy $(E_c - E)/J$ with $E - E_c \sim (T - T_c)^{1-\alpha}$, $E_c = -1.885$ and $\alpha = 0.32$.

but this is based on a theoretical argument which is only valid at low temperatures. We could not observe the boundaries of this phase in the Monte Carlo simulation, because the transition happens at very low temperatures and simulating the modified KDP model poses technical problems for the Monte Carlo procedure.

In the experiments with $CsOH.H_2O$ no ordering of the protons was observed,

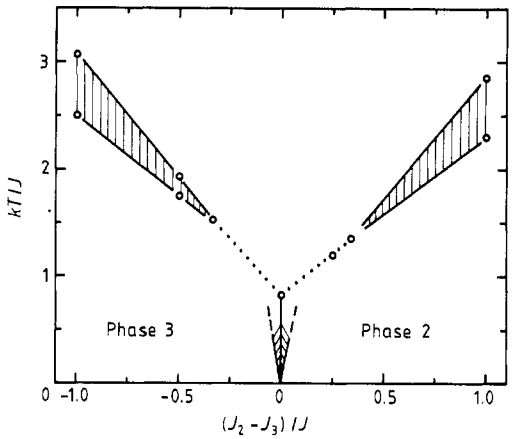

Figure 12. Phase diagram along the line $J_1 = -2(J_2 - J_3) = \text{constant}$ obtained by Monte Carlo simulations ($J = J_2 + J_3$). The dotted lines refer to second-order transitions and the full lines refer to Kosterlitz–Thouless transitions with a critical phase in between. At low temperatures there is a mixed phase as explained in § 3.

possible ordering of the protons could be very low as in KOH-doped ice (Leadbetter *et al* 1984). If the system is in a 'vertex-phase' as described in § 3 then it is difficult to find an order parameter which is also experimentally accessible.

Acknowledgments

We thank Dr T T Truong for valuable discussions and comments. We also thank Professor J Kanamori for discussions and for showing us his unpublished analysis of the ground states for a Kagome–Ising model, which also includes a fourth coupling constant J_4.

References

Barber M N 1982 *Phase Transitions and Critical Phenomena* vol 8, ed C Domb and J L Lebowitz (New York: Academic) p 146
Barber M N and Selke W 1982 *J. Phys. A: Math. Gen.* **15** L617
Baxter R J 1982 *Exactly Solved Models in Statistical Mechanics* (New York: Academic)
Binder K 1979 *Monte Carlo Methods in Statistical Physics* (Berlin: Springer)
Brandt U and Stolze J 1986 *Z. Phys.* B **64** 481
Challa M S S and Landau D P 1986 *Phys. Rev.* B **33** 437
dos Santos R R and Sneddon L 1981 *Phys. Rev.* B **23** 3541
Jose J V, Kadanoff L P, Kirkpatrick S and Nelson D R 1977 *Phys. Rev.* B **16** 1217
Kanamori J 1966 *Prog. Theor. Phys.* **50** 1426
—— 1985 *Ann. Phys., Paris* **10** 43
Kano K and Naya S 1953 *Prog. Theor. Phys.* **10** 158
Landau D P 1983 *Phys Rev.* B **27** 5604
Leadbetter A J, Ward R C, Clark J W, Tucker P A, Matsuo T and Suga H 1984 *J. Chem. Phys.* **82** 424
Lieb E H and Wu F Y 1972 *Phase Transitions and Critical Phenomena* vol 1, ed C Domb and M S Green (New York: Academic) p 321
Matsuo T and Suga H 1981 *Rev. Inorg. Chem.* **3** 371
Stahn M, Lechner R E, Dachs H and Jacobs H E 1983 *J. Phys. C: Solid State Phys.* **16** 5073
Sütö A 1981 *Z. Phys.* B **44** 121

Villain J and Bak P 1981 *J. Physique* **42** 657
Wannier G H 1950 *Phys. Rev.* **79** 357
Wu F Y 1967 *Phys. Rev. Lett.* **18** 605
Yeomans J M 1984 *Physica* **127B** 187